Symmetry-breaking commensurate states in generalised Frenkel-Kontorova models

1989 J. Phys.: Condens. Matter 1 2179

(http://iopscience.iop.org/0953-8984/1/12/003)

J. Phys.: Condens. Matter 1 (1989) 2179–2198. Printed in the UK

Symmetry-breaking commensurate states in generalised Frenkel–Kontorova models

Kazuo Sasaki† and Luis M Floria‡
Department of Physics, Carnegie-Mellon University, Pittsburgh, Pennsylvania 15213, USA

Received 18 July 1988

Abstract. Ground states of classical, one-dimensional systems consisting of atoms connected with harmonic springs subject to a periodic, symmetric potential are studied. It is shown that some choices of the periodic potential yield periodic (commensurate) ground states lacking the reflection symmetry of the Hamiltonian. The phase diagram of the ground states of a specific model which exhibits asymmetric commensurate phases is studied in detail. The transition from an asymmetric commensurate state to an incommensurate state is mediated by two types of solitons (discommensurations), while that from a symmetric one is mediated by a single type of soliton. Solitons are symmetric or asymmetric depending on the model parameters. First- and second-order transitions between symmetric and asymmetric states with the same period occur as the strength of the potential is varied. The soliton that mediates transitions from a commensurate to an incommensurate state changes its character infinitely many times as a first-order transition line is approached.

1. Introduction

Spatially modulated structures are often found in condensed-matter systems, such as atomic monolayers on crystal surfaces, magnetic systems and charge-density-wave systems (Bak 1982). One of the simplest theoretical models that produces such structures consists of a classical atomic chain, in which atoms are connected with harmonic springs, subject to a periodic potential. The energy (Hamiltonian) of the model is given by

$$H = \sum_n [\tfrac{1}{2}(u_n - u_{n-1} - \gamma)^2 + V(u_n)] \tag{1.1}$$

where u_n is the position of the nth atom, γ is the natural length of the spring and

$$V(u + 1) = V(u) \tag{1.2}$$

is the periodic potential. The model (1.1) with a sinusoidal V is often called the Frenkel–Kontorova model (Frenkel and Kontorova 1938). The first term in (1.1) favours a uniform structure with atomic spacing γ, while the second term forces the atoms to sit as close as possible to the minima of the potential. As a result of the competition between these two energies, the system finds a spatially modulated structure as a minimum-energy state (ground state). The structure is said to be commensurate if u_n modulo 1 is

† Permanent address: Department of Engineering Science, Faculty of Engineering, Tohoku University, Sendai 980, Japan.

‡ Permanent address: Instituto de Ciencias de los Materiales de Aragon, CSIC-Universidad de Zaragoza, 50015 Zaragoza, Spain.

0953-8984/89/122179 + 20 $02.50

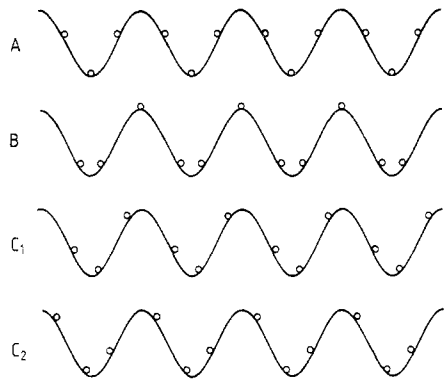

Figure 1. Spatially modulated structures of period 3 in generalised Frenkel–Kontorova models, (1.1) and (1.2).

a periodic function of n, and to be incommensurate otherwise.

Figure 1 schematically shows possible modulated structures with period 3. The ground state of type-A structure is seen, for example, in the Frenkel–Kontorova model. The type-B ground state, which is characterised by the presence of atoms at maxima of the potential, is found in the model with V a cosine plus a small second-harmonic term with the proper sign when the strength of the potential is weak (Griffiths and Chou 1986, Chou and Griffiths 1986). In this model a first-order transition from type-B to type-A ground states is observed when the potential strength is increased (Griffiths and Chou 1986, Chou and Griffiths 1986). One expects the type-C structure (C_1 and C_2 in figure 1) when $V(u)$ is an asymmetric function. In this paper we show that asymmetric, type-C ground states appear even when the potential is symmetric:

$$V(u) = V(-u). \tag{1.3}$$

If this is the case, two distinct phases, one of which is the mirror image of the other, can coexist (e.g. C_1 and C_2 in figure 1).

It is known (Aubry 1983a, Aubry and Le Dearon 1983) that in most cases a commensurate ground state of (1.1) is stable over a finite interval of γ. The commensurate state is unstable against the creation of defects (solitons or discommensurations) outside this interval. When the commensurate ground state is symmetric (type A or B), a soliton energy becomes zero at an edge of the interval, while the sum of energies of two distinct solitons becomes zero in the case of an asymmetric commensurate state (see § 2).

We study the phase diagram of the ground states of a specific model which exhibits asymmetric commensurate states by using the method of effective potentials (Griffiths and Chou 1986, Chou and Griffiths 1986) and other methods (§ 4). Numerical solutions to the non-linear eigenvalue equation of the method of effective potentials are obtained by employing a new algorithm (Floria and Griffiths 1988) which yields exact results for a discretised version of the equation (§ 3). Solitons that cause the instability of commensurate states are symmetric or asymmetric depending on the location in the phase diagram. In § 5 we discuss under what conditions asymmetric ground states of period 2 appear for a certain class of potential V.

2. Commensurate states with and without symmetry

2.1. Ground states

In this section we discuss some of the general properties associated with commensurate states of (1.1) with periodic, symmetric V (i.e. $V(u)$ satisfies (1.2) and (1.3)). Any such

a function $V(u)$ can be expressed by a Fourier cosine series:

$$V(u) = [K/(2\pi)^2] \sum_{k=1}^{\infty} \varepsilon_k [1 - \cos(2\pi k u)] \qquad (\varepsilon_1 = 1). \tag{2.1}$$

We assume $K > 0$. If the ε_k ($k > 1$) are not too large, $V(u)$ has one absolute minimum at $u = 0$ (modulo 1) and one absolute maximum at $u = \frac{1}{2}$ (modulo 1) in each period. In the following we assume this is the case, except in § 5.

A configuration $\{u_n\}$ is *commensurate* if there are irreducible, positive integers P and Q such that for any integer n,

$$u_{n+Q} = P + u_n \tag{2.2}$$

where Q is the period of the structure. The average atomic spacing ω defined by

$$\omega = (u_{n+Q} - u_n)/Q \tag{2.3}$$

is a rational number P/Q. We call ω the *winding number*.

A commensurate state $\{u_n\}$ of period Q is called *type A* (cf figure 1), if there exist integers r and s such that for any integer n,

$$u_{r+n} - s = s - u_{r-n} \qquad (Q \text{ odd}) \tag{2.4}$$

$$u_{r+n} - s = s - u_{r+1-n} \qquad (Q \text{ even}). \tag{2.5}$$

For Q odd there are atoms at minima of the potential V, while there are no atoms at minima of V for Q even. A commensurate state $\{u_n\}$ is called *type B* (cf figure 1), if there exist integers r and s such that for any integer n,

$$u_{r+n} - (s + \tfrac{1}{2}) = (s + \tfrac{1}{2}) - u_{r-n}. \tag{2.6}$$

In type-B configurations there are atoms at maxima of the potential V. A periodic configuration $\{u_n\}$ that does not satisfy any of (2.4)–(2.6) is called *type C* (cf figure 1). Both type-A and type-B configurations have reflection symmetry, while type-C configurations are asymmetric.

It is convenient to introduce the *phase* x of a commensurate configuration $\{u_n\}$, which plays the role of an order parameter to distinguish distinct ground states with the same winding number. The phase x of a configuration $\{u_n\}$ of period Q is defined by

$$x = (1/Q) \sum_{i=-(Q-1)/2}^{(Q-1)/2} u_{n+i} - \omega n \qquad (Q \text{ odd}) \tag{2.7}$$

$$x = (1/Q) \sum_{i=-Q/2+1}^{Q/2} u_{n+i} - \omega n \qquad (Q \text{ even}). \tag{2.8}$$

Note that x does not depend on the choice of the integer n in (2.7) or (2.8). Intuitively, x represents 'the centre-of-mass coordinate of a unit cell'. From the definitions (2.4)–(2.8), one find that $x = 0$ (modulo $1/Q$) for type-A states and $x = 1/2Q$ (modulo $1/Q$) for type-B states.

The energy associated with the order parameter x, which is the analogue of the Landau free energy, may be introduced as follows (Aubry 1983b). Find a minimum-energy configuration of period Q under the constraint that the phase variable x defined by (2.7) and (2.8) is fixed. The 'Landau potential' $U(x)$ is the energy per particle of the configuration thus found. Because $V(u)$ is periodic and symmetric, $U(x)$ is also periodic and symmetric:

$$U(x + 1/Q) = U(x) \tag{2.9}$$

$$U(-x) = U(x). \tag{2.10}$$

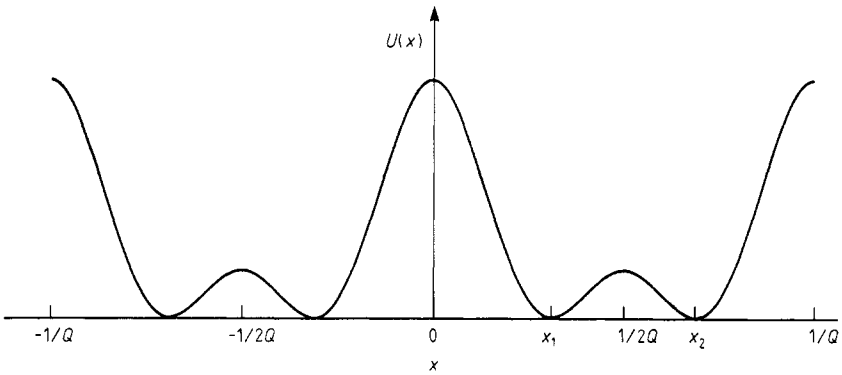

Figure 2. A 'Landau potential' $U(x)$ which yields commensurate ground states without reflection symmetry.

The period of $U(x)$ is $1/Q$, since a configuration $\{u_n\}$ with phase x has the same energy as the shifted configuration $\{u_n + 1\}$ with phase $x + 1$ and the renumbered configuration $\{u_{n+1}\}$ with phase $x + \omega$, where $\omega = P/Q$ is the winding number (Aubry 1983b). The absolute minima of $U(x)$ correspond to (degenerate) commensurate ground states. If $U(x)$ has only one absolute minimum per period, equation (2.10) implies the ground state is either type A ($x = 0$) or type B ($x = 1/2Q$). It should be noted, however, that $U(x)$ can have, in general, more than one minimum per period. If it has two minima, for example, as schematically shown in figure 2, ground states of type C are realised. The configuration corresponding to the minimum x_2 in figure 2 is a mirror image of the one corresponding to x_1. Although Aubry pointed out the possible existence of such ground states, he had no examples and claimed such a situation is exceptional (Aubry 1983a).

2.2. *Solitons (discommensurations)*

A commensurate state is stable over a finite interval of the parameter γ, provided that the corresponding $U(x)$ is not a constant. Outside the interval the commensurate state is unstable against creation of solitons (discommensurations). A *soliton* configuration $\{u_n\}$ is a local minimum-energy configuration (any local perturbation cannot decrease the energy) which approaches two distinct ground states $\{u_n^+\}$ and $\{u_n^-\}$ asymptotically:

$$u_n \to u_n^{\pm} \qquad \text{as } n \to \pm\infty. \tag{2.11}$$

The phases x^+ and x^- corresponding to $\{u_n^+\}$ and $\{u_n^-\}$ are locations of two neighbouring minima of the Landau potential $U(x)$. What we call solitons here correspond to what Aubry calls elementary discommensurations (see for example theorem 3 of Aubry (1983a)). When $x^- < x^+$ ($x^- > x^+$), the configuration $\{u_n\}$ is called an *advanced* (a *retarded*) *soliton*. It is clear from figure 2 that there are two types of advanced (retarded) solitons associated with asymmetric commensurate states: One corresponds to a soliton with $x^- = -x_1$ and $x^+ = x_1$ ($x^- = x_1$ and $x^+ = -x_1$), and the other with $x^- = x_1$ and $x^+ = x_2$ ($x^- = x_2$ and $x^+ = x_1$). The situation is quite analogous to the (continuum) double-sine–Gordon model with two types of solitons (Condat *et al* 1983, DeLeonardis and Trullinger 1983).

The creation energy E of a soliton $\{u_n\}$, which satisfies (2.11), with respect to the underlying commensurate ground state may be calculated by

$$E = \lim_{p,q\to\infty} (1/Q) \sum_{r=q+1}^{q+Q} \sum_{n=-p+1}^{r} [K(u_n, u_{n-1}) - K(u_n^-, u_{n-1}^-)] \tag{2.12}$$

where

$$K(u, u') = \tfrac{1}{2}(u - u' - \gamma)^2 + V(u) \tag{2.13}$$

and Q is the period of the ground state†. Note that the quantity

$$\sum_{n=-p+1}^{r} [K(u_n, u_{n-1}) - K(u_n^-, u_{n-1}^-)] \tag{2.14}$$

does not, in general, converge as $r \to \infty$; it oscillates as a function of r for large r. We therefore need the second summation in (2.12), which averages out the oscillation. The soliton energy (2.12) depends linearly on γ, and the coefficient of the linear dependence is given by the 'phase shift' associated with the soliton:

$$\partial E/\partial \gamma = x^+ - x^- \tag{2.15}$$

where x^+ and x^- are the phases of two ground states $\{u_n^+\}$ and $\{u_n^-\}$. The formula (2.15) is derived from equations (2.7), (2.8) and (2.12) and the fact that the stationary configurations $\{u_n\}$, $\{u_n^+\}$ and $\{u_n^-\}$ are independent of γ (this is because the force equilibrium equations $\partial H/\partial u_n = 0$, which all stationary configurations satisfy, does not depend on γ). From the arguments in the previous paragraph, the right-hand side of (2.15) is found to be $-1/Q$ $(+1/Q)$ for an advanced (a retarded) soliton if the ground state is symmetric. If E in the left-hand side of (2.15) is replaced by the sum of energies of two advanced (retarded) solitons of different types, in the case of asymmetric ground states, the right-hand side will be $-1/Q$ $(+1/Q)$.

A commensurate state with winding number ω is stable as long as the energies of solitons created on it are positive. Equation (2.15) shows this to be true over a finite interval of γ, $\gamma^-(\omega) < \gamma < \gamma^+(\omega)$. If the ground state is symmetric, the right (left) edge of the interval, γ^+ (γ^-), is the point at which the energy of advanced (retarded) soliton, E^+ (E^-), is zero: $E^+ < 0$ $(E^- < 0)$ for $\gamma > \gamma^+$ $(\gamma < \gamma^-)$. As γ is increased from $\gamma^+(\omega)$, the ground state changes its configuration whose winding number increases continuously (theorem 9 of Aubry (1983a)). The ground-state configuration for γ slightly larger than $\gamma^+(\omega)$ can be viewed as a periodic (or quasi-periodic) array of advanced solitons in the background of the commensurate structure of winding number ω. If the commensurate ground state is asymmetric, the edges of the interval, γ^+ and γ^-, over which this state is stable are determined by the conditions

$$E_1^+ + E_2^+ = 0 \qquad \text{at } \gamma = \gamma^+ \tag{2.16}$$

$$E_1^- + E_2^- = 0 \qquad \text{at } \gamma = \gamma^-. \tag{2.17}$$

Here E_1^+ (E_1^-) and E_2^+ (E_2^-) are the energies of two different types of advanced (retarded) solitons (type 1 and type 2). We note that one of E_1^+ and E_2^+, say E_1^+, is negative and the other is positive at $\gamma = \gamma^+$ (the same is true at $\gamma = \gamma^-$); E_1^+ is negative over a finite portion of the interval $\gamma^- < \gamma < \gamma^+$. The negative energy of one type of soliton does not imply any phase transition, because if one tries to put a finite density of type-1 solitons (which have negative energies) one is forced to introduce the same amount of type-2 solitons (topological constraint). Therefore, the phase transition occurs when (2.16) is satisfied.

† Tang (1987) and Tang and Griffiths (1988) give an expression for the energy of a 'defect' $\{u_n\}$ whose limiting configurations $\{u_n^+\}$ and $\{u_n^-\}$ are 'phase shifted' from each other, i.e. they are related by $u_n^+ = u_{n+r}^- + s$ with some integers r and s; their expression is therefore applicable to a soliton created on a symmetric commensurate state. Equation (2.12), which applies to a soliton created on an asymmetric commensurate state as well, is equivalent to their expression in the case of a symmetric ground state.

3. The method of effective potentials

3.1. Formalism

In this section the essentials of the method of effective potentials are explained. The method provides the ground-state energy, the ground-state configuration and some information about soliton excitations. The exposition will be intuitive rather than rigorous. A more complete introduction can be found in the original papers (Griffiths and Chou 1986, Chou and Griffiths 1986). Although the applicability of the method of effective potentials extends to more general models, the following presentation is centred on the model (1.1), where, for the sake of brevity, $W(x-y)$ will denote the energy of a harmonic spring joining atoms placed at locations x and y.

Consider a semi-infinite chain of atoms extending to the left placed in the periodic potential V. The location of the right-most atom is held fixed at u while the other atoms are allowed to relax to a state of minimum energy. Let us call $R(u)$ the 'effective potential' acting on the right-most atom, so that $R'(u)$ is the force that must be externally applied to hold the end atom at position u. The position of the atom next to the right-most one is given by u', which minimises $W(u-u')+R(u')$, so that the 'right' effective potential $R(u)$ satisfies the equation

$$\lambda + R(u) = V(u) + \min_{u'}[W(u-u') + R(u')] \tag{3.1}$$

where λ is a constant. We consider (3.1) as an eigenvalue equation, where we impose the periodicity condition

$$R(1+u) = R(u). \tag{3.2}$$

The eigenvalue λ turns out to be the energy per atom in the ground state.

Analogously, for the left-most atom in a semi-infinite chain extending to the right, the 'left' effective potential $S(u')$ satisfies the equation

$$\lambda + S(u') = V(u') + \min_{u}[W(u-u') + S(u)] \tag{3.3}$$

and the periodicity condition

$$S(1+u') = S(u'). \tag{3.4}$$

The 'total' effective potential $F(u)$ experienced by an atom in a doubly infinite chain is

$$F(u) = R(u) + S(u) - V(u) \tag{3.5}$$

where $V(u)$ is subtracted to avoid double counting.

Once the eigenvalue equation (3.1) is solved, the ground-state configuration is obtained as follows. The map $\tau(u)$, associated with a solution R of (3.1), assigns to each position u the point u' (not unique, in general) at which the minimum on the right-hand side is achieved. The map $\sigma(u')$, associated with a solution S of (3.3), is defined in a similar way. An infinite sequence of points $\{u_n\}$, $n \leqslant p$, is an R *half-orbit* provided

$$u_{n-1} \in \tau(u_n) \qquad \text{for all } n \leqslant p. \tag{3.6}$$

Similarly $\{u_n\}$, $n \geqslant q$, is an S *half-orbit* if

$$u_{n+1} \in \sigma(u_n) \qquad \text{for all } n \geqslant q. \tag{3.7}$$

A doubly infinite sequence $\{u_n\}$ is an R *orbit* if (3.6) holds for all integers and it is an S *orbit* if (3.7) holds for all integers. The attractor of the map τ (σ) is an R (S) orbit. An R

orbit is always a ground state and, for a given periodic ground state, there is an R satisfying the minimisation eigenvalue equation (3.1) such that the given periodic ground state is the associated R orbit. The same statements hold for S orbits.

Assuming that V and W are continuous functions, it can be shown that there is some continuous and periodic function R which satisfies (3.1) and that the corresponding λ is unique for a given V and W. Even if V and W have continuous first derivatives, the effective potentials can, in general, have 'upward kinks', i.e. points in which the first derivatives decrease discontinuously. These upward kinks correspond to discontinuities in the corresponding map.

If the potential $V(u)$ is symmetric, i.e. satisfies (1.3), a solution to (3.3) can be constructed from a solution to (3.1), or vice versa, by setting

$$S(u) = R(-u) \tag{3.8}$$

and the corresponding S orbit is the mirror image of the R orbit.

Although this method is valid for commensurate and incommensurate states, we are considering only commensurate (periodic) ground states and, however degenerate, we will call a ground state *unique* when all other ground states can be obtained from it by translation and/or relabelling, i.e. by transformations $u_n \rightarrow u_{n+r} + s$ with some integers r and s. A ground state of type C is not unique because its mirror image cannot be obtained from it by those transformations. In the following a ground state of type C will be denoted by C_1 and its mirror image by C_2.

If the ground state is unique (state of type A or B) the absolute minima of the effective potential $F(u)$ are located at the points belonging to the ground-state configuration. When the ground state is of type C there are two effective potentials $F_1(u)$ and $F_2(u)$ corresponding to the two ground states C_1 and C_2:

$$F_\alpha(u) = R_\alpha(u) + S_\alpha(u) - V(u) \tag{3.9}$$

where $\alpha = 1$ or 2, and R_α and S_α are the solutions of (3.1) and (3.3) for the ground state C_α. The ground state C_α is an R_α and S_α orbit, and the absolute minima of F_α correspond to the locations of atoms in the ground state C_α. Since C_2 is the mirror image of C_1, the following relations between the effective potentials hold:

$$R_\alpha(u) = S_\beta(-u) \qquad F_\alpha(u) = F_\beta(-u) \tag{3.10}$$

where $\alpha, \beta = 1, 2$ $(\alpha \neq \beta)$.

If γ is close enough to the edge of stability (γ^+ or γ^-) of a unique periodic ground state, several secondary minima other than the absolute ones appear in the potential F; see figure 5 below. Those points belong to the soliton configuration (advanced or retarded) and the soliton energy is given by

$$E = F(u_s) - F(u_0) \tag{3.11}$$

where u_0 is any point in the ground state and u_s is any point of the secondary minima of F. This formula is obtained from (2.12) and the fact that the soliton configuration is an R half-orbit and an S half-orbit.

If γ is close enough to the edge of stability (γ^+ or γ^-) of a type-C periodic ground state, there appear infinitely many secondary minima in the potential F_α ($\alpha = 1$ or 2); see figure 6 below. The locations of those minima correspond to a configuration with two solitons infinitely far apart. The two solitons are advanced solitons of different types if γ is close to γ^+, or retarded solitons of different types if γ is close to γ^-. The formula (3.11) with F replaced by F_α gives the sum of the energies of the two solitons, which can

be used to calculate the phase boundary of a type-C ground state.

The information about a single soliton, in the case of a type-C ground state, can be obtained from a 'mixed' effective potential defined by

$$F_{\alpha\beta}(u) = R_\alpha(u) + S_\beta(u) - V(u) \qquad (\alpha \neq \beta). \tag{3.12}$$

If γ is close enough to the edge of stability (γ^+ or γ^-) of a type-C periodic ground state, the absolute minima of $F_{\alpha\beta}(u)$ sit on the points belonging to the corresponding (advanced or retarded) soliton configuration, which tends towards C_α to the left and towards C_β to the right. The soliton energy is calculated from (2.12) and the fact that the soliton configuration is an R_α half-orbit and an S_β half-orbit:

$$E_{\alpha\beta} = F_{\alpha\beta}(u_s) - Q^{-1} \sum_{i=1}^{Q} [R_\alpha(u_i^\alpha) + S_\beta(u_i^\beta) - V(u_i^\beta)] \tag{3.13}$$

where u_s is any point in the soliton configuration, Q is the period of the ground-state configuration and u_i^β ($i = 1, \ldots, Q$) are points in the C_β ground state.

3.2. Numerical method

Analytical solutions to the minimisation eigenvalue equation (3.1) can be found in some special cases (see § VID of Chou and Griffiths (1986)) but in general this highly non-linear equation must be solved numerically. For this purpose it is convenient to replace W in (3.1) and (3.3) by the periodic function

$$W^*(y) = \min_m W(m + y) \tag{3.14}$$

where m is integer, so that one may restrict the position of the atoms to the inverval $0 \leq u < 1$. We shall impose a grid of n points in the unit interval and solve the discretised equation

$$\lambda + x(j) = \min_i [K(j, i) + x(i)] \tag{3.15}$$

where

$$K(j, i) = V(v_j) + W^*(v_j - v_i) \qquad i, j = 1, 2, \ldots n, \quad v_i, v_j \in [0, 1). \tag{3.16}$$

The formal analogy of (3.15) with the eigenvalue problem in linear algebra is apparent if one replaces sum by product and $\min_i$ by Σ_i. Cuninghame-Green (1979) has developed the algebraic theory for such operations and, in fact, equation (3.15) is an example of the eigenvalue problem in minimax algebra. This author has shown that the eigenvalue λ is unique and is equal to the minimum over all cyclic averages of the form

$$\langle K \rangle_C = p^{-1} \sum_{m=1}^{p} K(j_m, j_{m+1}) \tag{3.17}$$

where C is a cycle: $j_1, j_2, \ldots, j_{p+1} = j_1$. In terms of our original (however discretised) physical problem, the minimising cycle corresponds to the ground-state configuration, whose energy per particle is the eigenvalue λ. A path from j_0 to j_m is a finite sequence of points $j_0, j_1, \ldots, j_m$. The length of this path is m and its weight is defined as

$$\sum_{r=0}^{m-1} K(j_r, j_{r+1}).$$

The most efficient algorithms for computing optimal cycles (Karp 1978, von Golitschek 1982) exploit the idea that a path (long enough) of minimal weight must contain

an optimal cycle. The algorithm described below is a modification of von Golitschek's algorithm and computes the minimum cyclic mean λ, a minimising cycle and the corresponding eigenvector $x(i)$.

In what follows, L is an upper bound for λ, J is a subset of $N = \{1, 2, \ldots, n\}$, $y(j)$ is real-valued and $\tau(j)$ is an integer-valued function. A prime, as in J' or $y'(j)$, denotes a new value (or set) produced by the algorithm. If C is a cycle, $j_1, j_2, \ldots, j_{p+1} = j_1$, we say that $y(j)$ is consistent on C provided

$$y(j_m) + L = K(j_m, j_{m+1}) + y(j_{m+1}) \tag{3.18}$$

where L is the average of this cycle. (Note that on a one-cycle $C = j_1$, any $y(j_1)$ is consistent.)

Step 0 (initialisation). Calculate the averages of all one- and two-cycles and let L be the minimum of them, and C a cycle where this minimum is achieved. Let $y(j) = +\infty$ for j not in C, and choose $y(j)$ consistently on C. Let $\tau(j) = 0$ (a dummy value) for j not in C, $\tau(j_1) = j_1$ if $C = j_1$ is a one-cycle, and $\tau(j_1) = j_2$, $\tau(j_2) = j_1$ if $C = (j_1, j_2)$ is a two-cycle. Let J consist of the elements in C.

Step 1. For j from 1 to n, let

$$y'(j) = \min[y(j), K(j, i) + y(i) - L; \text{ for all } i \in J]. \tag{3.19}$$

If $y'(j) < y(j)$, let $\tau(j) = i$, for some i where the minimum in (3.15) occurs. After the $y'(j)$ have been calculated, let

$$J' = \{j : y'(j) < y(j)\}. \tag{3.20}$$

If $J' = \varnothing$, then stop. If J' is not empty, set $J = J'$, $y(j) = y'(j)$, for all i, and go to step 2.

Step 2. Look for a cycle C' of the τ map (i.e. some j such that $\tau(\ldots(\tau(j))\ldots) = j$), for which L' is less than L. If such a cycle is found, let $L = L'$, $C = C'$ and return to step 1.

When this algorithm stops, L is equal to λ, the minimising cyclic average, and C is a minimising cycle. If L has the same value as in step 0, $y(j)$ is the eigenvector associated with this cycle. If L has decreased, an additional computation is required, as follows: Let $y(j) = +\infty$ at all points not in the minimising cycle C. Choose $y(j)$ consistently on C and let $\tau(j) = 0$ for all j not in C. Then iterate step 1 without performing step 2, until the stop condition ($J' = \varnothing$) is satisfied; at this point, $y(j)$ is the required eigenvector and $\tau(j)$ is the associated map, in the sense that for all j, $\tau(j)$ is a value of i at which the minimum on the RHS of (3.15) is achieved.

The observed dependence on the running time of the algorithm on the number n of grid points is about n^2. Typical values for the CPU time of a run for a grid of 1000 points are about 10 min on a microVAX (about 1 min on a VAX 11/870) for a FORTRAN-coded program. In general, much coarser (for example 100 points) grids give a sufficiently good approximation to the potentials for most purposes (a few seconds on a microVAX).

4. Phase diagram for a specific model

4.1. Phase diagram

We find that some of the potentials $V(u)$, (2.1), with third or fourth harmonics yield asymmetric commensurate ground states. In this section we shall study the phase diagram

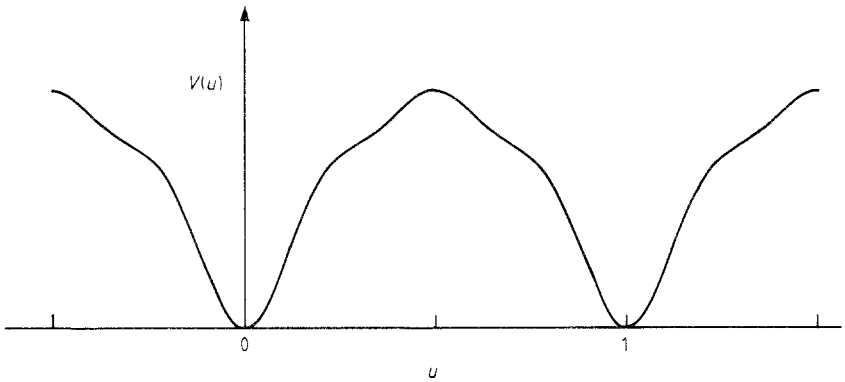

Figure 3. The periodic potential $V(u)$ given by (2.1) with $\varepsilon_2 = \frac{1}{4}$, $\varepsilon_3 = \frac{1}{6}$ and $\varepsilon_k = 0$ $(k \geq 4)$.

for one such model: the model with the periodic potential (2.1) in which

$$\varepsilon_2 = \tfrac{1}{4} \qquad \varepsilon_3 = \tfrac{1}{6} \qquad \text{and} \qquad \varepsilon_k = 0 \ (k \geq 4). \tag{4.1}$$

The function $V(u)$ has convex portions around $u \simeq \pm 0.35$ (modulo 1) as seen in figure 3. This structure seems to help the appearance of asymmetric ground states. We note, however, that such a structure is not essential; even infinitesimally small ε_2 and ε_3 can yield asymmetric commensurate states (see § 5).

Figure 4 shows a portion of the phase diagram in the γ–K plane for the model (4.1), obtained by the method of effective potentials. A rough phase diagram was first obtained by finding ground-state configurations at various points in the γ–K plane. At this stage a few hundred grid points per unit interval were used. Then more precise locations of the phase boundaries were determined by calculating the energies of appropriate solitons from the effective potentials obtained with 1000 grid points per unit interval. For example, figure 5 shows the effective potential $F(u)$ defined by (3.5) associated with a symmetric ground state of $\omega = \frac{1}{3}$ at $K = 1.2$, $\gamma = 0.3775$, obtained with 1000 grid points. The locations of the three absolute minima give the locations of atoms (modulo 1) in the ground state. The relative height of the secondary minima with respect to the absolute minima gives the creation energy of an advanced soliton, from which the phase boundary

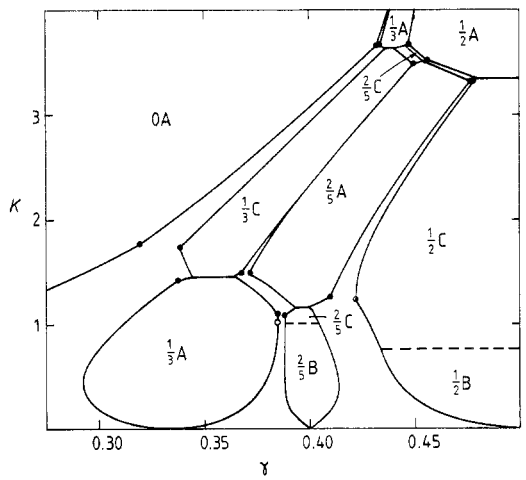

Figure 4. The phase diagram in the γ–K plane for the model (4.1).

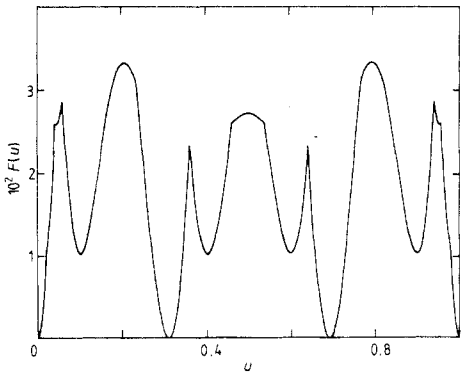

Figure 5. The effective potential $F(u)$ associated with a symmetric ground state of period 3 defined by (3.5), calculated at $K = 1.2$, $\gamma = 0.3775$.

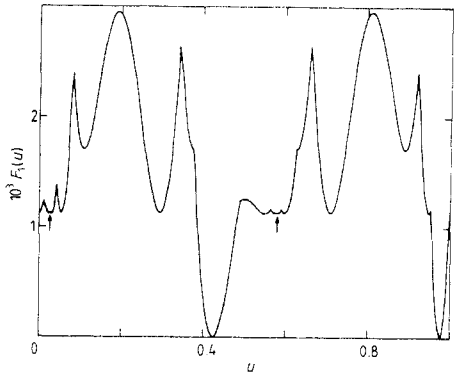

Figure 6. The effective potential $F_1(u)$ associated with an asymmetric ground state of period 2 defined by (3.9), calculated at $K = 1.2$, $\gamma = 0.425$. There are infinitely many secondary minima, which accumulate to the points indicated by the arrows.

$\gamma^+(\frac{1}{3})$ is calculated as described in § 2. An example of the effective potential $F_1(u)$ defined by (3.9) associated with a symmetry-breaking ground state of period 2 is shown in figure 6, calculated at $K = 1.2$, $\gamma = 0.425$, with 1000 grid points. The locations of the two absolute minima give the locations of atoms (modulo 1) in the ground state. The secondary minima (infinitely many, with equal height) correspond to a configuration with two retarded solitons of different types infinitely far apart. The relative height of the secondary minima with respect to the absolute minima gives the sum of the energies of the two solitons, for which the phase boundary $\gamma^-(\frac{1}{2})$ is calculated as described in § 2.

Several locations of the boundaries of the $\omega = 0$ and $\omega = \frac{1}{2}$ phases thus obtained were compared with those obtained from more precise calculations of soliton energies based on the solutions to the force equilibrium equations

$$\partial H/\partial u_n = 0. \tag{4.2}$$

The comparison of the two results at several locations shows that the errors in the results of the method of effective potentials with 1000 grid points are more or less of order 10^{-5} in γ.

Only a few commensurate phases are shown in figure 4. Unmarked regions are occupied by (infinitely many) other commensurate states and incommensurate states. The numbers in the figure represent the winding numbers and the symbols A, B and C indicate the types of ground states as discussed in § 2. The horizontal bars separate phases of the same winding number but different types. The order parameter x defined in (2.7) and (2.8) changes discontinuously (continuously) when a solid (broken) horizontal bar is crossed. For this specific model (4.1) all the observed transitions between A and C phases are discontinuous ('first-order' transitions), whereas those between B and C are continuous ('second-order' transitions). No transitions between A and B are observed in this model.

As in the case of the model studied by Griffiths and Chou (1986) and Chou and Griffiths (1986) in which commensurate states of type A and type B appear, there are accumulation points of horizontal bars in the γ–K plane for our model. They found some such points on the boundaries of the $\omega = 0$ and the $\omega = \frac{1}{2}$ phases (see figure 5 of Griffiths and Chou (1986) or figure 15 of Chou and Griffiths (1986)). They further noticed that

Figure 7. Configurations of the advanced soliton in the $\omega = 0$ phase for different values of K.

these points occur at the same value of K at which the minimum-energy soliton in the corresponding $\omega = 0$ and $\omega = \frac{1}{2}$ phases changes its character, and that the phase boundary has discontinuous slope at these points. In figure 4 some such special points in our model are shown by full and open circles found by observing changes in the character of appropriate solitons, which will be discussed in the next subsection. The phase boundary has discontinuous slope at full circles, which are accumulation points of solid horizontal bars, and has continuous slope at open circles, which are accumulation points of broken horizontal bars.

4.2. Changes in the character of solitons

The configurations of the minimum-energy soliton in the $\omega = 0$ phase for $K = 3.7$, 2.0 and 1.0 are shown in figure 7. The soliton for K larger than $K_0 = 3.66204$ (the upper accumulation point on the boundary of the $\omega = 0$ phase shown in figure 4) is symmetric; that for $K_0 > K > K_1 = 1.77485$ (the lower accumulation point) is asymmetric, with one atom in the convex part of $V(u)$ near the top of the potential. The symmetric (asymmetric) soliton exists even for $K < K_0$ ($K > K_0$) as a metastable state but has higher energy than the asymmetric (symmetric) soliton. The change in character of the minimum-energy soliton is of first order in that its energy has discontinuous slope at $K = K_0$, which yields the discontinuous slope of the phase boundary. The minimum-energy soliton for $K < K_1$ is again symmetric.

Now we discuss the soliton in the $\omega = \frac{1}{2}$ phase. Let us first consider the soliton in the A phase ($K > K_c = 3.34731$). The minimum-energy retarded soliton above the uppermost accumulation point is symmetric, as schematically shown in figure 8(a); below this point it is asymmetric, figure 8(b); it becomes symmetric again, figure 8(c), when the second accumulation point is passed from above; and so on. In addition to the changes in symmetry, it is noticed that the 'core' of the soliton expands each time an accumulation point is passed from the higher K side. It is likely that there are a series of

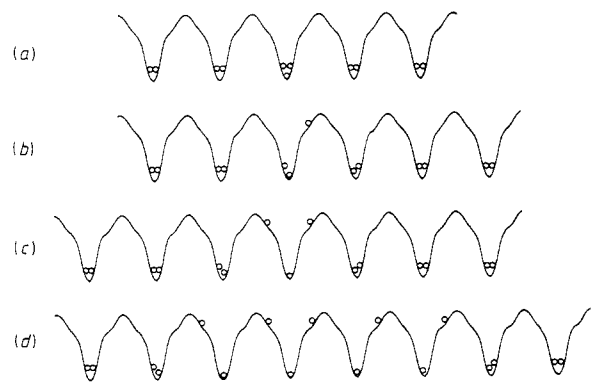

Figure 8. Changes in the character of the retarded soliton in the $\frac{1}{2}$A phase.

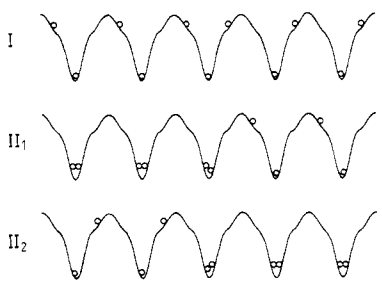

Figure 9. The three retarded solitons on the horizontal bar at $K = 3.34731$ in the $\omega = \frac{1}{2}$ phase.

accumulation points and they accumulate to the left edge of the horizontal bar in the $\omega = \frac{1}{2}$ phase at $K = K_c$ (the existence of the accumulation point of accumulation points was suggested by Griffiths and Chou (1986)). The core of the soliton will grow larger and larger as K_c is approached. We shall show this is actually the case.

On the 'coexistence line' $K = K_c$, A and B phases have the same energy per atom, and there are three types of retarded solitons (the Landau potential $U(x)$ introduced in § 2 has three absolute minima in each period). They are shown in figure 9. The soliton in the $\frac{1}{2}$A phase can be viewed as a bound state of these three solitons with II_1 to the left of I and II_2 to the right of I. The change in the character of the soliton corresponds to the change in the distances between constituent solitons. For the first three configurations of the soliton in figure 8, this view point may not be clear. However, as the core of soliton expands, this viewpoint becomes easier to see (e.g. figure 8(*d*)). If the distances d_1 and d_2 between solitons of type I and type II_1 and between type I and type II_2 respectively are large enough, the energy of the soliton in the A phase as a bound state of the three constituent solitons may be expressed as

$$E(d_1, d_2) = (\gamma - \gamma_c)/2 + a\exp(-bd_1) + a\exp(-bd_2) \qquad (K = K_c) \tag{4.3}$$

at $K = K_c$. Here $\gamma_c = 0.48039$ is the left edge of the horizontal bar at $K = K_c$, and a and b are positive constants. The first term in (4.3) is the sum of the energies of the three constituent solitons; this quantity has linear dependence in γ and is zero at $\gamma = \gamma_c$, as seen from the general arguments in § 2. The second and third terms are the two-body interaction energies. The interaction between solitons I and II_1 has the same distance dependence as that between I and II_2, because the soliton I is symmetric and the soliton II_1 is the mirror image of the soliton II_2. It can be shown (Tang 1987, Yokoi *et al* 1988) that for the present model the interaction is repulsive and decays exponentially as the distance increases. It is somewhat ambiguous how to define the distance between solitons. We use a convention such that $d_1 = 2$ and $d_2 = 3$ for the configuration in figure 8(*d*). If one knows the configurations of isolated solitons I and II_2, the constants a and b can be evaluated (Tang 1987). We obtain $a = 6.3847 \times 10^{-3}$ and $b = 3.8615$ by solving the force equilibrium equations (4.2) for these soliton configurations.

The energy of the soliton in the $\frac{1}{2}$A phase is larger than (4.3) for $K > K_c$; the configuration in the core of the soliton looks very much like that of the C phase, and the C phase has higher energy per atom than the A phase. Slightly above K_c the soliton energy would be

$$E(d_1, d_2) = \varepsilon(2d - \nu)(K - K_c) + (\gamma - \gamma_c)/2 + a\exp(-bd_1) + a\exp(-bd_2) \tag{4.4}$$

where $d = d_1 + d_2$ and $\varepsilon(K - K_c)$ is the difference of the energies per atom in the C and A phases. The constant ε is found to be 1.6253×10^{-2} from the energy calculations of the C and A phases near K_c. The parameter ν (constant) is introduced to take account of the K dependence of the energies of the constituent solitons in the vicinity of K_c.

If one accepts the phenomenological expression (4.4) for the soliton energy, the minimun-energy soliton is found by minimising (4.4) with respect to d_1 and d_2 under the constraint that d_1 and d_2 are integers. The minimum of (4.4) is achieved when $d_1 = d_2$, and the d_1 minimising (4.4) increases in a stepwise manner as $K - K_c$ is decreased; d_1 increases from N to $N + 1$ at $K = K_N$, where K_N is calculated from (4.4) as

$$K_N - K_c = (a/2\varepsilon)(1 - \mathrm{e}^{-b})\,\mathrm{e}^{-bN}. \tag{4.5}$$

The minimum-energy soliton is thus predicted to change its character infinitely many times as K_c is approached. The boundary of the $\frac{1}{2}$A phase is given by $E(d_1, d_2) = 0$. γ_N,

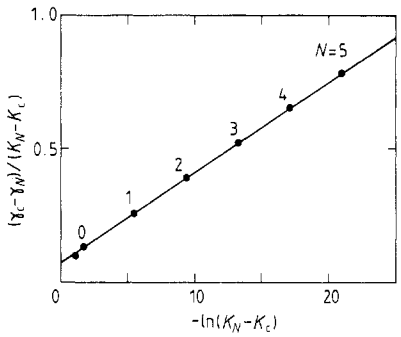

Figure 10. The points (γ_N, K_N) on the boundary of the $\frac{1}{2}$A phase at which the minimum-energy soliton changes its character. The straight line is the prediction (4.7) of the phenomenological theory.

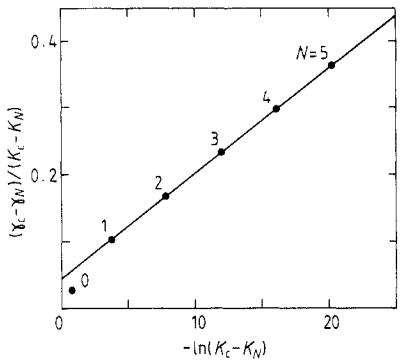

Figure 11. The points (γ_N, K_N) on the boundary of the $\frac{1}{2}$C phase at which the minimum-energy soliton of type II changes its character. The straight line is the prediction of the phenomenological theory.

the value of γ corresponding to K_N on the boundary, is calculated from (4.4) as

$$\gamma_c - \gamma_N = 2a\,e^{-bN}[(1 - e^{-b})(2N - \nu/2) + 2]. \tag{4.6}$$

Therefore, these points (γ_N, K_N) on the boundary accumulate to the point (γ_c, K_c) according to

$$\gamma_c - \gamma_N = \alpha(K_N - K_c)[-\ln(K_N - K_c) + \beta] \tag{4.7}$$

where α and β are constants: $\alpha = 8\varepsilon/b = 0.033672$ and β is expressed in terms of a, b, ε and ν.

The above phenomenological argument fails to explain the appearance of the asymmetric soliton ($d_1 \neq d_2$) like the one in figure 8(b) ($d_1 = 0$, $d_2 = 1$). This is because we have neglected the three-body interaction among the constituent solitons. The three-body interaction is much smaller (Szpilka and Fisher 1986, Fisher and Szpilka 1987) than the pair interaction for large d_1 and d_2, although it cannot be neglected for small d_1 and d_2. Actually, the results of the method of effective potentials show that the segments of the phase boundary where the minimum-energy soliton is asymmetric shrink rapidly as K_c is approached. The predictions (4.5)–(4.7) are concerned with the asymptotic region where such segments are negligibly small.

For quantitative comparison between the 'theory' and 'experiment', we evaluated the soliton energy from the numerical solution to the force equilibrium equations (4.2) to find the precise locations at which the change in character occurs. We find good agreement with (4.5) for $N \geqslant 3$ (relative error less than 10^{-4}). From the fit of the data with (4.6), the unknown parameter in the 'theory' is found to be $\nu = 0.1206$. The numerical data for (γ_N, K_N) are plotted in figure 10 as suggested by the prediction (4.7), where β is calculated to be 2.179 by using the value of ν obtained above. There are a pair of data points for each value of N because of the existence of the asymmetric soliton. Only one ($N = 0$) of the pairs is separable in the figure. The lowest point in the figure corresponds to the uppermost point on the boundary of the $\frac{1}{2}$A phase in figure 4. Figure 10 clearly shows that the asymptotic behaviour of the change in the character of the soliton is correctly described by the simple phenomenological theory.

The boundary of the $\frac{1}{2}$C phase near K_c can be studied in a similar way but with a slight modification. In this phase there are two types of retarded solitons; one of them changes

its character infinitely many times as K_c is approached, while the other does not. The latter soliton is essentially the same as the type-I soliton in figure 9. The former can be viewed as a bound pair of type-II_1 and type-II_2 solitons with type II_2 to the left of type II_1. The core of this type-II composite soliton looks like the configuration of the $\frac{1}{2}$A phase, and it expands as K_c is approached. The same phenomenological argument as before can be applied and we obtain the following expression for the sum of the energies of type-I and type-II solitons:

$$E_I + E_{II}(d) = \varepsilon(2d - 1 + \nu)(K_c - K) + (\gamma - \gamma_c)/2 + a' \exp(-b'd) \tag{4.8}$$

where d is the distance between the constituent solitons in the type-II soliton defined with a similar convention to the one we have used to define d_1 and d_2 for the soliton in the $\frac{1}{2}$A phase. The constants ε and ν are the same as before, whereas a' and b' in the interaction term are new ones: $a' = 5.0732 \times 10^{-2}$ and $b' = 4.1314$ as calculated from the configurations of the isolated constituent solitons at $K = K_c$. The locations (γ_N, K_N) on the phase boundary at which the type-II soliton changes its character (d increases from N to $N + 1$ as K is increased) predicted from (4.8) satisfies equations similar to (4.5)–(4.7). The locations (γ_N, K_N) numerically evaluated from the explicit calculations of the soliton energies agree well with the 'theoretical' predictions as before (relative error less than 10^{-4} for $N \geq 2$). The numerical data are plotted in figure 11, which again shows that the asymptotic behaviour is correctly described by the simple phenomenological theory. (The lowest data point in the figure corresponds to the lowest full circle on the boundary of the $\frac{1}{2}$C phase in figure 4.)

The phenomenological theory can be applied to describing the change in the character of the soliton in the vicinity of any of the solid horizontal bars in the phase diagram, figure 4. The same is true for the model studied by Griffiths and Chou (1986) and Chou and Griffiths (1986) mentioned earlier.

The change in the character of the soliton at an open circle in figure 4 is more delicate than that at a full circle. We found only one such a point at $K = 1.026$ on the boundary of the $\frac{1}{3}$A phase. (We do not know whether there are other such points.) Below this point the advanced soliton in the $\frac{1}{3}$A phase is symmetric with an atom (at the centre of the soliton) right on the top of the potential V. As this point is passed from below, the atom at the centre moves off from the symmetry point of the potential continuously and the soliton becomes asymmetric. The soliton energy changes continuously and smoothly. The change in the character of the soliton is of 'second order'. (The asymmetric soliton is no longer a minimum-energy soliton above the full circle at $K = 1.092$, but exists as a metastable one. The minimum-energy soliton is now symmetric, with no atom at a symmetry point of the potential V in the core of the soliton.)

5. When does the symmetry-breaking state appear?

As we have seen, there exists a potential $V(u)$ in the model (1.1) that yields symmetry-breaking ground states. What conditions should $V(u)$ satisfy to have asymmetric commensurate states? We shall partially answer this question by considering the $\omega = \frac{1}{2}$ phase for a limited class of $V(u)$.

If both the type-A and type-B configurations are unstable, the ground state must be asymmetric. We therefore start with the stability analysis of the type-A and type-B structures of period 2. This may be done by studying the Landau potential $U(x)$ introduced in § 2. For the case of period 2 it is given by

$$U(x) = [V(x + \xi) + V(x - \xi)]/2 + 2(\xi - \tfrac{1}{4})^2 + (\gamma - \tfrac{1}{2})^2/2 \tag{5.1}$$

where $\xi(x)$ is defined as a solution of

$$V'(x+\xi) - V'(x-\xi) + 8\xi - 2 = 0 \tag{5.2}$$

V' being the derivative of V. The locations of atoms u_1 and u_2 in a 'unit cell' are related with x and ξ: $u_1 = x - \xi$ and $u_2 = x + \xi$. If (5.2) has more than one solution for a given x, ξ is understood to be the solution that yields the minimum of (5.1). In any case the ξ must satisfy, at least, the condition of local minimum energy for a given x:

$$V''(x+\xi) + V''(x-\xi) + 8 > 0. \tag{5.3}$$

For x corresponding to a stationary configuration (a configuration satisfying the force equilibrium equations (4.2)) $U'(x) = 0$. This configuration is unstable if $U''(x) < 0$ and (locally) stable if $U''(x) > 0$. From (5.1) and (5.2) we have

$$U''(x) = \frac{2[V''(u_1) + V''(u_2)] + V''(u_1)V''(u_2)}{4 + [V''(u_1) + V''(u_2)]/2}. \tag{5.4}$$

Note that the denominator in (5.4) is always positive, owing to the condition (5.3). For the A phase ($x = 0$) (5.4) yields $U''(0) = V''(u_1)$.

Using the formula (5.4) one can argue to some extent the relation between the stability of the A and B states of period 2 and the functional form of $V(u)$, but we will be more specific. We consider the potential (2.1) with $\varepsilon_k = 0$ ($k \geqslant 4$), the model studied in § 4 being a specific example of this class (the class of potentials with $\varepsilon_k = 0$ ($k \geqslant 3$) was studied by Chou and Griffiths (1986)). Applying (5.4) to this class of potentials, one finds that the B state ($x = \frac{1}{4}$, $\xi = \frac{1}{4}$) is unstable for $K > K_B$, given by

$$K_B = 16\varepsilon_2/[(1+9\varepsilon_3)^2 - (4\varepsilon_2)^2] \tag{5.5}$$

when $\varepsilon_2 > 0$ and $(1+9\varepsilon_3)^2 > (4\varepsilon_2)^2$, and that it is always unstable when $\varepsilon_2 < 0$. When $V(u)$ has no secondary minima, the A phase is unstable for $K < K_A$ and $\varepsilon_2 > 0$ where K_A is given by

$$K_A = (1 - 4u_0)/[V'(u_0)/K] \tag{5.6}$$

and u_0 is determined by $V''(u_0) = 0$ ($0 < u_0 \leqslant \frac{1}{4}$). For a potential $V(u)$ such that $K_A > K_B$ the ground state must be asymmetric at least for $K_A > K > K_B$. The parameter values (4.1), for example, realise this situation. There exist the parameters $\varepsilon_2 < 0$ and $\varepsilon_3 > 0$ such that $V''(u) = 0$ has two real solutions for u in the interval $(0, \frac{1}{4})$; we denote these solutions by u_- and u_+ ($u_- < u_+$). In this situation the A state is unstable for $K_+ < K < K_-$ provided that $K_+ < K_-$, where

$$K_\pm = (1 - 4u_\pm)/[V'(u_\pm)/K]. \tag{5.7}$$

Therefore, the ground state must be of type C for intermediate strength of the potential (remember that the B state is unstable for $\varepsilon_2 < 0$).

Even when one or both of the A and B states are (locally) stable the symmetry-breaking, C-type ground state can appear. For detailed investigation of when the C phase of period 2 appears, we have made combined use of the stability analysis and the method of effective potentials. Figure 12 summarises the results of the investigation. A point in the ε_2–ε_3 plane specifies a potential $V(u)$. For the potential corresponding to a point $(\varepsilon_2, \varepsilon_3)$ in the region marked by the symbol [B, C.A] in figure 12, for example, the second-order transition from the B to C phases and then the first-order transition to the A phase occurs as the strength of the potential, K, is increased. The period (comma) in the symbol indicates that the transition is of first (second) order. For potentials in the

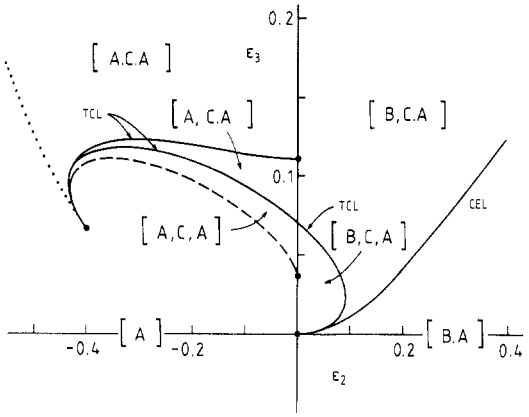

Figure 12. Types of phases of period 2 realised by the class of potentials with second (ε_2) and third (ε_3) harmonics for the potential corresponding to a point (ε_2, ε_3) in the region marked by [B, C.A], for example, the ground-state changes from type B to type C through the second-order transition and then to type A through the first-order transition as the strength of the potential is increased. The line $\varepsilon_2 = 0$ is one of the boundaries separating different regions.

upper region in the ε_2–ε_3 plane there appear asymmetric ground states at intermediate strength of the potential; for those in the lower right region, [B.A], the first-order transition from the B to A phases occurs as K is increased; for those in the lower left region, [A], only the A phases are obtained. The line $\varepsilon_2 = 0$ is one of the boundaries separating different regions. The boundaries marked by TCL are projections of the tricritical lines in the ε_2–ε_3–K space onto the ε_2–ε_3 plane, and the one marked by CEL is the projection of the line of critical end points (Griffiths 1975). These features can be seen more clearly in an intersection of the phase diagram in the ε_2–ε_3–K space with a plane of ε_2 = constant. For instance, see figure 13. In figure 13 the full (broken) lines indicate that the transition between the two phases separated by the line is of first (second) order. The nature of the transition (first- or second-order) between the A and C phases changes at a tricritical point (TCP), figures 13(b)–(d). The second-order transition line (or the line of critical points) between the B and C phases terminates at a critical end point (CEP), figures 13(a) and (b).

The boundary lines in figure 12 are obtained as follows. The critical end line is the intersection of the three surfaces (see figures 13(a) and (b)): one surface is given by $U(0) = U(\frac{1}{4})$, the boundary between the A and B phases; another is the boundary between the B and C phases, which is given by $K = K_B$ where K_B is defined in (5.5). The critical end line is obtained by solving these two equations simultaneously. The tricritical line is a line on the boundary between the A and C phases (see figures 13(b)–(d)) at which the nature of the transition changes. The portion corresponding to the second-order transition of the phase boundary is given by $U''(0) = 0$ and $U^{(4)}(0) > 0$, where

$$U^{(4)}(0) = V^{(4)}(\xi) - 3[V^{(3)}(\xi)]^2/[4 + V''(\xi)] \tag{5.8}$$

is the fourth derivative of U at $x = 0$. In (5.8) ξ is the solution of (5.2) for $x = 0$. The tricritical line is obtained by solving $U''(0) = 0$ and $U^{(4)}(0) = 0$ simultaneously. The first equation is equivalent to $K = K_A$ for $\varepsilon_2 > 0$ and $K = K_\pm$ for $\varepsilon_2 < 0$, where K_A and $K_\pm$ are defined in (5.6) and (5.7). The broken curve in figure 12 is given by the condition $u_+ = u_-$, where $u_\pm$ are the solutions to $V''(u) = 0$ as defined above (5.7). This condition leads to

$$768\varepsilon_2^2 = -3(1 - 14\eta + \eta^2) \pm (5 + \eta)[3(3 - \eta)(1 + 5\eta)]^{1/2} \tag{5.9}$$

and $2\varepsilon_2 > -\eta$, where $\eta = 27\varepsilon_3$. The dotted curve corresponds to the common asymptote of the two first-order transition lines in figure 13(e). On this line $V(u)$ has three absolute

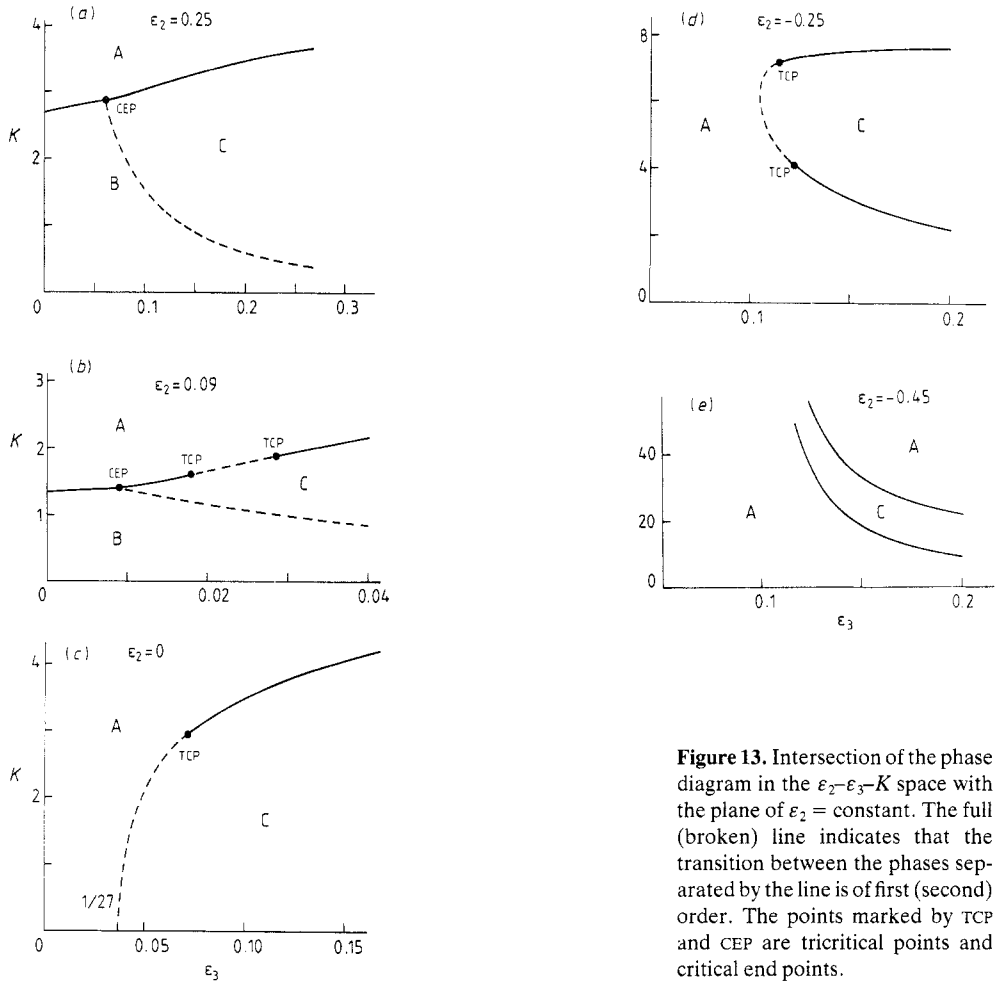

Figure 13. Intersection of the phase diagram in the ε_2–ε_3–K space with the plane of ε_2 = constant. The full (broken) line indicates that the transition between the phases separated by the line is of first (second) order. The points marked by TCP and CEP are tricritical points and critical end points.

minima per period (at the right end of the line, $(\varepsilon_2, \varepsilon_3) = (-\frac{2}{5}, \frac{1}{15})$, the three minima collapse); above the line it has one absolute minimum at $u = 0$; below the line it has two at finite u. This line is given by $\varepsilon_3 = \varepsilon_2^2/4(1 + \varepsilon_2)$ and $\varepsilon_2 \leqslant -\frac{2}{5}$.

We have considered only the commensurate phase of period 2. The same analysis can be done, in principle, for other commensurate phases, although the analysis will be more complicated for longer-period phases. One will find different conditions for asymmetric ground states of different winding numbers to appear.

6. Concluding remarks

We have demonstrated the existence of symmetry-breaking commensurate states in generalised Frenkel–Kontorova models (1.1) with periodic, symmetric substrate potentials $V(u)$. The existence of such structures is not obvious. The phase diagram for a specific model has been studied in detail. The horizontal bars (the first-order transition lines) in figure 4 are analogous to the ones obtained by Aubry *et al* (1985) and by Griffiths and Chou (1986) and Chou and Griffiths (1986), while the broken horizontal bars

(the second-order transition lines) seem to have no analogous examples in models of commensurate–incommensurate transitions studied previously.

We note that symmetry-breaking commensurate states can be found also in previously studied models. There are at least two such models. One is the model (1.1) in which V is a piecewise parabolic function with continuous derivative (Bullett 1986, Chou and Griffiths 1986). For special choice of the parameter γ and the strength of V, the model yields 'sliding' commensurate states (invariant circles); in other words the Landau potentials $U(x)$ introduced in § 2 are independent of x. In such a circumstance the configuration corresponding to any value of x is a ground state and it is asymmetric for almost all x. The piecewise parabolic nature of V seems crucial for the occurrence of sliding commensurate states. We claim that the symmetry-breaking state of this type is rather exceptional.

Another example is an exactly solvable model for a ferroelectric system in an electric field studied by Aubry *et al* (1985). The model is an extention of (1.1) such that the system has two sublattices. The Hamiltonian has reflection symmetry without an electric field, but some of commensurate states have asymmetric configurations. The existence of two sublattices is essential to the appearance of symmetry-breaking states in this model. These states exist independently of the strength of a periodic potential, in contrast to the case in the model (1.1).

As suggested by the phenomenological argument in § 4, the phenomenon of infinitely many changes in the character of solitons (discommensurations) seems to be a universal feature associated with the first-order transition between phases with the same period but different symmetries. The phenomenological theory predicts that the phase boundary in the vicinity of an end point of a solid horizontal bar is a portion of a polygon with infinitely many edges; the vertices of the polygon accumulate to the end point of the horizontal bar. The phase boundaries for the model of Aubry *et al* (1985) mentioned above, in an electric field, have this property (see figures 6 and 7 in Aubry (1985)), which we think, can be understood by this picture of infinitely many changes in the character of solitons.

Recently, Yokoi (1988) has studied a specific example of the change in the character of solitons in the model with a second harmonic added to a sinusoidal potential, whose phase diagram was first worked out by Griffiths and Chou (1986). He considers the soliton in the $\omega = 0$ phase, and shows that the points on the phase boundary at which the soliton changes its character accumulate at $K = 0$, $\gamma = 0$. The way they accumulate is different from the result of our analysis in § 4 for the soliton in the $\omega = \frac{1}{2}$ phase: the values of K at which the soliton changes its character accumulate according to a power law $K_N \sim N^{-2}$ $(N \to \infty)$ in Yokoi's case, while they obey an exponential law, equation (4.5), in ours. The shapes of the phase boundaries are also different in the two cases: parabolic in Yokoi's analysis and linear with a logarithmic factor, equation (4.7), in ours. We suspect that Yokoi's analysis is relevant to the $\omega = 0$ phase but not to accumulation points on the other phase boundaries with horizontal bars.

Acknowledgments

We are much indebted to Professor R B Griffiths for stimulating discussions and encouragement. We would like to thank Kevin Bassler and Leihan Tang for helpful discussions on the topic of this paper and closely related matters. We also would like to thank Dr S Aubry for informative comments and for bringing Bullett's work to our attention. Particular thanks go to Kevin Bassler for his critical reading of the manuscript. This

work has been supported by the National Science Foundation under Grant No DMR-8613218. One of us (LMF) acknowledges the financial support of the NATO Scientific Program through a Postdoctoral Grant.

References

Aubry S 1983a *Physica* **7D** 240
—— 1983b *J. Physique* **44** 147
Aubry S, Axel F and Vallet F 1985 *J. Phys. C: Solid State Phys.* **18** 753
Aubry S and Le Dearon P Y 1983 *Physica* D **8** 381
Bak P 1982 *Rep. Prog. Phys.* **45** 578
Bullett S 1986 *Commun. Math. Phys.* **107** 241
Chou W and Griffiths R B 1986 *Phys. Rev.* B **34** 6219
Condat C A, Guyer R A and Miller M D 1983 *Phys. Rev.* B **27** 474
Cuninghame-Green R A 1979 *Minimax Algebra* (Berlin: Springer)
DeLeonardis R M and Trullinger S E 1983 *Phys. Rev.* B **27** 1867
Fisher M E and Szpilka A M 1987 *Phys. Rev.* B **36** 644
Floria L M and Griffiths R B 1988 *Preprint*
Frenkel J and Kontorova T 1938 *Phys. Z. Sowjetunion* **13** 1
Griffiths R B 1975 *Phys. Rev.* B **12** 345
Griffiths R B and Chou W 1986 *Phys. Rev. Lett.* **56** 1929
Karp R M 1978 *Discrete Math.* **23** 309
Szpilka A M and Fisher M E 1986 *Phys. Rev. Lett.* **57** 1044
Tang L 1987 *PhD Thesis* Carnegie-Mellon University
Tang L-H and Griffiths R B 1988 *Preprint*
von Golitschek M 1982 *Numer. Math.* **39** 65
Yokoi C S O 1988 *Phys. Rev. B* to be published
Yokoi C S O, Tang L-H and Chou W 1988 *Phys. Rev.* B **37** 2173